energies

MDPI

Review

A Review of Open-Access Image Datasets for Power Line Inspection

Xue-Hua Wu [1], Enze Zhao [1], Kangyao Yuan [1] and Yu-Qing Bao [2,*]

[1] School of Electrical Engineering, Nanjing University of Industry Technology, Nanjing 210023, China; wuxuehua@niit.edu.cn (X.-H.W.)
[2] School of Electrical Engineering and Automation, Nanjing Normal University, Nanjing 210023, China
* Correspondence: baoyuqing@njnu.edu.cn

Abstract

Automated power line inspection plays a crucial role in maintaining grid reliability within smart cities by identifying potential defects in towers, conductors, insulators, and fittings. While modern anomaly detection relies heavily on deep neural networks (DNNs), training these models requires massive amounts of high-quality image data. However, a significant scarcity of publicly available datasets persists because data acquisition not only demands highly specialized professional skills but also faces strict data protection regulations enforced by grid companies. To bridge this gap, this paper presents a comprehensive review of open-access image datasets dedicated to power line inspection. Based on strict inclusion criteria—specifically, unrestricted public availability and a direct focus on core power line components—19 datasets are systematically selected and analyzed. We provide a detailed taxonomy and comparative analysis of these datasets in terms of inspection targets, acquisition platforms, annotation toolkits, and labeling schemes. Furthermore, our investigation highlights current research trends and identifies critical gaps, such as the disproportionate focus on insulators and the notable scarcity of multimodal data. To address the limitations of small-scale datasets, we also discuss existing data augmentation strategies and synthetic data generation techniques. Ultimately, this review serves as a unified navigational guide, aiming to foster the development of more robust visual inspection algorithms and to inspire future high-quality dataset construction in the power domain.

Keywords: automated power line inspection; defect detection; public datasets; data augmentation

Check for updates

Academic Editor: Tek-Tjing Lie

Received: 19 April 2026
Revised: 26 May 2026
Accepted: 28 May 2026
Published: 30 May 2026

Copyright: © 2026 by the authors. Licensee MDPI, Basel, Switzerland. This article is an open access article distributed under the terms and conditions of the Creative Commons Attribution (CC BY) license.

1. Introduction

The dataset with numerical images is important for training the deep neural networks (DNNs). There are several famous public datasets for general-purpose recognition, such as Pattern Analysis, Statical Modeling, and Computational Learning Visual Object Classes (PASCALVOC); Microsoft Common Objects in Context (MS COCO); Open Images; and ImageNet [1–4]. However, the availability of real-world datasets for power line inspection remains limited. The datasets developed by utility companies are generally not released to the public due to privacy regulations and data protection laws [5].

Specifically, previous reviews have made noteworthy contributions by summarizing deep learning classification frameworks, discussing generic target detection models, and outlining the historical evolution of unmanned aerial vehicle (UAV) inspection modalities [6–20]. However, a critical methodological gap persists across these existing reviews, as they primarily focus on algorithm performance metrics while treating the underlying

 https://doi.org/10.3390/en19112649

data sources as a secondary concern. Most of these prior surveys only briefly list a handful of early baseline datasets, failing to provide a systematic evaluation of data-scaling boundaries, annotation paradigms, or target distribution imbalances. To bridge this knowledge gap and establish a rigorous benchmark for the community, this paper proposes a highly comprehensive review that moves beyond generic literature surveys to deeply dissect 19 open-access image datasets [21–85] dedicated to power line inspection. By expanding the investigation matrix to encompass these 19 representative repositories, we systematically map out their evolutionary trajectories, analyze their cross-dataset associations, and critically evaluate their structural bottlenecks across multiple granular dimensions, thereby establishing actionable guidelines for future data-centric paradigm shifts in power grid intelligence.

In order to provide valuable insights and practical guidelines, a comprehensive review and analysis of the open-access image datasets of power line inspection is conducted. To ensure a rigorous and reproducible selection process, we established explicit inclusion criteria (IC) and exclusion criteria (EC), as follows:

IC1 (Relevance): The dataset must specifically focus on overhead power lines and their core components (e.g., insulators, conductors, towers, or fittings).
IC2 (Open Access): The dataset must be publicly available and fully accessible on public repositories (e.g., GitHub, IEEE DataPort, Zenodo, Kaggle) for academic research.
IC3 (Scientific Support): The dataset must be accompanied by a peer-reviewed research publication or metadata feature description to verify its scientific validity.
EC1 (Data Modality): Datasets consisting entirely of non-image formats (e.g., text logs, pure numerical telemetry data) were excluded.
EC2 (Availability Failure): Datasets with permanently expired, broken, or replaced download links that could no longer be retrieved during our investigation were excluded.

Following a systematic search using the predefined keywords across platforms like Web of Science and Google Scholar, a total of 19 representative image datasets strictly satisfied all criteria and were selected for in-depth analysis.

The remainder of this paper is organized as follows: Section 2 provides the fundamentals of power line inspection, detailing the main components, potential faults, and typical imaging techniques. Section 3 conducts a comprehensive analysis of the currently available open-access datasets, systematically comparing them in terms of data sources, inspection targets, acquisition platforms, and annotation strategies. Finally, Section 4 concludes the paper, summarizing the core findings, discussing the persistent challenges in dataset construction, and outlining promising avenues for future research.

2. Power Line Inspection Fundamentals

Power line inspection is a vital process for maintaining grid reliability, primarily relying on visual observation to identify potential faults. Manual inspection has long been the predominant method for power line inspection, which can be categorized into ground inspection and airspace inspection. Ground inspection is conducted by teams on foot or in off-road vehicles utilizing tools like binoculars and infrared cameras for visual observation. Airspace inspection is conducted by teams with the assistance of helicopters. These primary approaches are labor-intensive, inefficient, and limited by harsh terrain and weather. Recently, wheeled robots, climbing robots, and multi-rotor UAVs have been widely applied to achieve automated inspection of power lines [6].

Multi-rotor UAVs have become the mainstream choice because they are cost-effective, highly flexible, and can capture high-resolution data from close range without damaging infrastructure. The popular inspection system typically consists of three components: an autofocus camera, a communication network, and a ground monitoring center. The

captured videos are transmitted through the communication network to the monitoring center, where detection algorithms process the data and display inspection results in real time. The inspection strategy between adjacent transmission towers is shown in Figure 1.

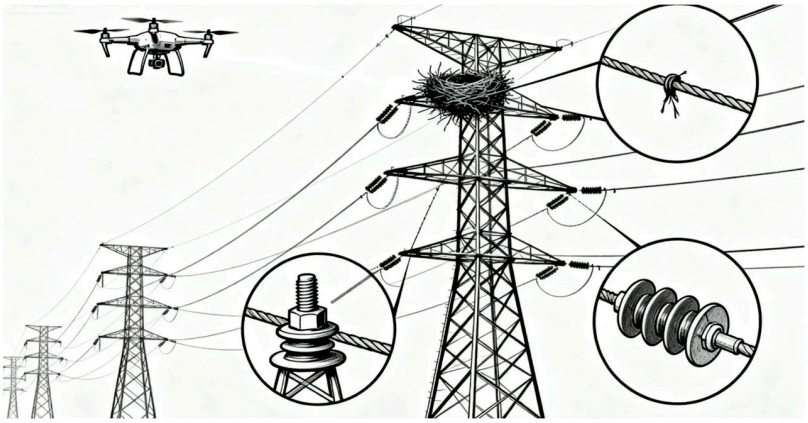

Figure 1. Power line inspection.

2.1. Power Line Components and Associated Faults

The main components of power transmission lines include insulators, towers, conductors, and various line fittings. Power line inspection is an essential task to ensure the safety of the power grid. Typically, the task of power line inspection consists of four major aspects: the inspection of insulators, inspection of power towers, inspection of conductors, and inspection of power line fittings. These inspections aim to identify potential defects, which are shown in Figure 2. Insulators require the detection of missing caps and contamination, as well as the leakage-current-induced heating that precedes flashover. Towers need assessing for corrosion, deformation, and loose connections that could lead to collapse. Foreign objects need to be detected due to their potential to cause power line faults. Conductors demand monitoring of strand breakage, sag, and overheating. Vegetation encroachment constitutes a routine item in power line inspection schedules. Fittings such as clamps, spacers, and dampers require identification of looseness, breakage, missing, and corrosion. The abnormal operating conditions of components can be automatically detected by deep learning algorithms [18–20].

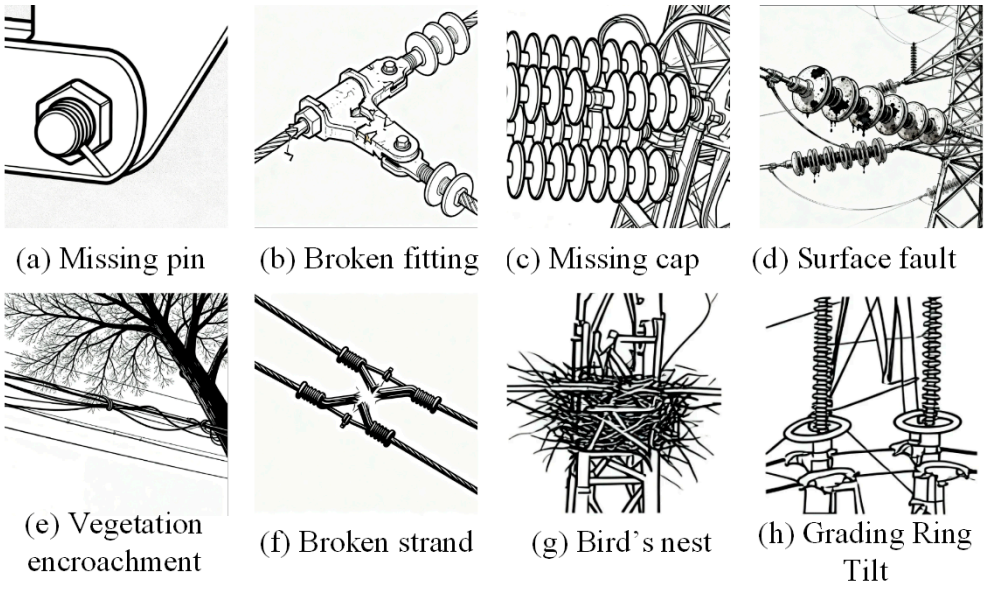

Figure 2. Samples of potential defects.

2.2. Typical Inspection Imaging Techniques

A range of imaging techniques is utilized in power line inspection, including visible light imaging [9], infrared imaging [10,11], ultraviolet (UV) imaging [12–14], light detection and ranging (LiDAR) imaging [15,16], and X-ray imaging [17]. As shown in Figure 3, visible light imaging delivers essential data for routine monitoring, whereas the complementary techniques afford a more detailed assessment of component health. Infrared imaging leverages thermal signal differences to eliminate complex background interference and effectively identify thermal anomalies such as overheating or overloading inside components. UV imaging enables the early detection of hidden electrical defects by observing corona discharge, but its application is constrained by limited effective range and high equipment costs. LiDAR generates high-precision 3D structural maps using laser pulses, remains unaffected by light fog or rain, and is particularly suitable for accurately detecting vegetation encroachment and physical obstacles. X-ray imaging can penetrate materials for in-depth internal structure diagnostics. However, due to the risk of ionizing radiation, high equipment cost, and the need for professional operation, its use in routine inspection is significantly limited.



Figure 3. Visible light imaging of ID-2024 insulator defect dataset.

3. The Investigation of Image Datasets

In this study, 19 publicly available image datasets are examined. These datasets have played a vital role in providing diverse images of power lines to improve the accuracy of power line inspections. The size of each dataset, along with the year it was made publicly available, is presented in Figure 4. A comprehensive summary of each dataset is shown in Table 1.

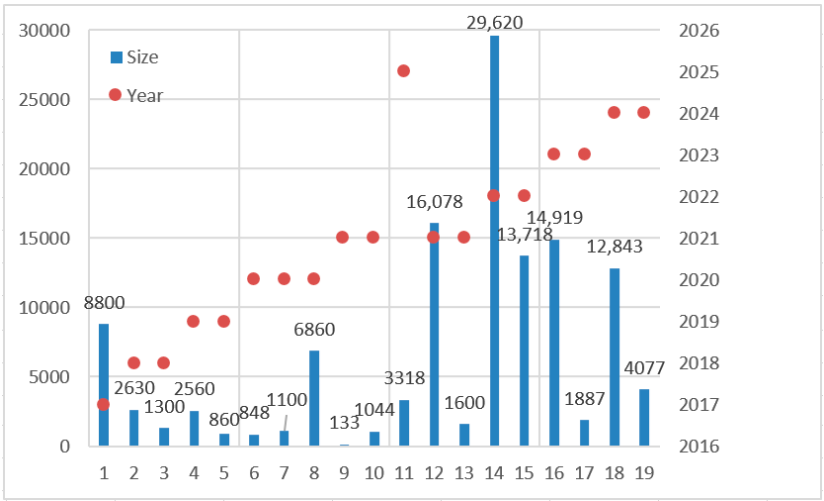

Figure 4. Size and year of the datasets.

Table 1. Summary of publicly available datasets in power line inspection.

Dataset		Year	Location	Type	Target	Platform	Size	Annotation	Link
Yetgin's IR and VL aerial image dataset [21–29]		2017	Turkey	RGB and IR 128 × 128	Conductor	Helicopter	8800	Pixel-wise BMP format	[22–26]
Tomaszewski's insulator dataset [30–32]		2018	Poland	RGB 2400 × 1600	Insulator	Dedicated system	2630	——	[33]
Bian's power transmission tower (PTT) dataset [34–36]		2018	China	RGB multi-scale	Tower	DJI Matrice 100	1300	Bounding box VOC2007 format	[37]
Prates's overhead power distribution lines (OPDL) dataset [38,39]		2019	Brazil	RGB Not given	Conductor	Dedicated system	2560	——	[40]
Zhang's power line detection in unmanned aerial vehicle (PLD-UAV) dataset [41–43]		2019	China	RGB 540 × 360	Conductor	DJI Phantom 4 Pro	860	Bounding box MAT format	[44]
Tao's Chinese power line insulator dataset (CPLID) [45–47]		2020	China	RGB 1152 × 864	Insulator	DJI Matrice 200	848	Bounding box VOC2007 format	[48,49]
Abdelfattah's transmission towers/power line aerial image (TTPLA) dataset [50]		2020	USA	RGB 3840 × 2160	Tower, and conductor	Parrot-ANAFI	1100	Pixel-wise COCO format	[51,52]
Federal University of Pernambuco power line dataset	André L.'s unifying public datasets for insulator (UPID) [53]	2020	China	RGB 1152 × 864	Insulator	Albumentations API	6860	Bounding box COCO format	[53]
	André L.'s STN power line assets dataset (STN PLAD) [54,55]	2021	Brazil	RGB 5472 × 3078 or 5472 × 3648	Tower, insulator, spacer, damper, and plate	DJI Phantom 4 Pro	133	Bounding box COCO format	[56–59]
Federal University of Juiz de Fora power transmission line (PTL) dataset	Diniz's power transmission line dataset [60,61]	2021	Brazil	RGB 1920 × 1088 or 320 × 240	Conductor	DJI Tello drone/Parrot Bebop 1 drone	1044	——	[60]
	Pussente's power transmission line dataset [62,63]	2025	Brazil/ China/ USA	RGB 640 × 640	Conductor	Parrot Bebop 2 drone	3318	Bounding box YOLOv8 format	[64,65]
Diwakar's power line detection dataset [66]		2021	Indian	RGB 128 × 128	Conductor	UAV unknown	16,078	Classification label CSV format	[66]
The Electric Power Research Institute (EPRI) electric utility infrastructure imagery	EPRI insulator defect image dataset (IDID) [67]	2021	USA	RGB multi-scale	Insulator	UAV unknown	1687	Bounding box JSON format	[68]
	EPRI distribution inspection imagery [68]	2022	USA	RGB 5184 × 3888	Tower, insulator, conductor, and transformer	UAV unknown	29,620	Pixel-wise CSV format	[69,70]
Zhang's synthetic foggy insulator dataset (SFID) [71]		2022	China	RGB 1152 × 864	Insulator	Albumentations API FINet	13,718	Bounding box COCO format	[72]

Table 1. *Cont.*

Dataset		Year	Location	Type	Target	Platform	Size	Annotation	Link
Savva's aerial power infrastructure detection dataset [73]		2023	Cyprus	RGB multi-scale	Tower	DJI Matrice 300 RTK	13,831	Bounding box YOLO/ COCO/VOC format	[74]
Guangxi University insulator dataset	Shuang's RSIn-dataset [75–77]	2023	China	RGB 1152 × 864 to 7360 × 4912	Insulator	DJI Matrice 300 RTK	1887	——	[78]
	Cui's diverse insulator dataset (DINS) [79]	2024	China	RGB Not given	Insulator	Not given	12,843	Bounding box VOC format Pixel-wise PNG format	[80,81]
Lu's ID-2024 insulator defect dataset [82–84]		2024	China	RGB multi-scale	Insulator	DJI Mini 2 SE model drone	1631	Bounding box TXT format	[85]

3.1. Data Source Characteristics

The fundamental characteristics of the original data dictate the upper performance limits of deep learning models in power line inspection. To provide a systematic taxonomy of the data sources, we critically analyze the 19 reviewed datasets from three primary dimensions: data provenance and inter-dataset associations, geospatial distribution, and image resolution trade-offs.

3.1.1. Data Provenance and Inter-Dataset Associations

Tracing the provenance of these datasets reveals a distinct evolutionary trend from independent real-world acquisitions to derived and synthetic expansions. As shown in Figure 5, early datasets, such as Yetgin's IR and VL dataset, Tomaszewski's insulator dataset, and Prates's OPDL dataset, were independently constructed from scratch using helicopters or dedicated laboratory systems. However, acquiring images of defective components in real-world operational scenarios poses immense safety and logistical challenges. Consequently, recent efforts have shifted toward data derivation and synthetic generation to expand existing benchmarks. For instance, the UPID dataset was not captured independently but was systematically generated by applying advanced data augmentation techniques (via the Albumentations API) to Tao's pioneering CPLID. Taking this a step further, Zhang's SFID utilized a Foggy Insulator Network (FINet) to synthetically inject diverse fog conditions into the UPID dataset. This strong inter-dataset association highlights a paradigm shift: researchers are increasingly relying on synthetic generation and augmentation to overcome the inherent scarcity of real-world defective samples.

3.1.2. Geospatial Distribution and Environmental Bias

The geospatial origin of a dataset profoundly impacts the environmental diversity of its backgrounds, encompassing variations in vegetation, terrain, and climate. As illustrated in Figure 6, the geographic distribution of the 19 datasets is highly skewed. They originate from only seven countries, with China accounting for the largest proportion, followed by Brazil and the United States. While this concentration reflects active research communities and robust grid infrastructure in these regions, it inherently introduces an environmental bias. Datasets collected in specific geographical zones may lack diverse weather patterns, seasonal changes, or unique architectural backgrounds found globally. This geospatial imbalance could potentially hinder the cross-domain generalization capability of trained

models when deployed in unseen environments, underscoring the pressing need for more globally collaborative dataset construction.

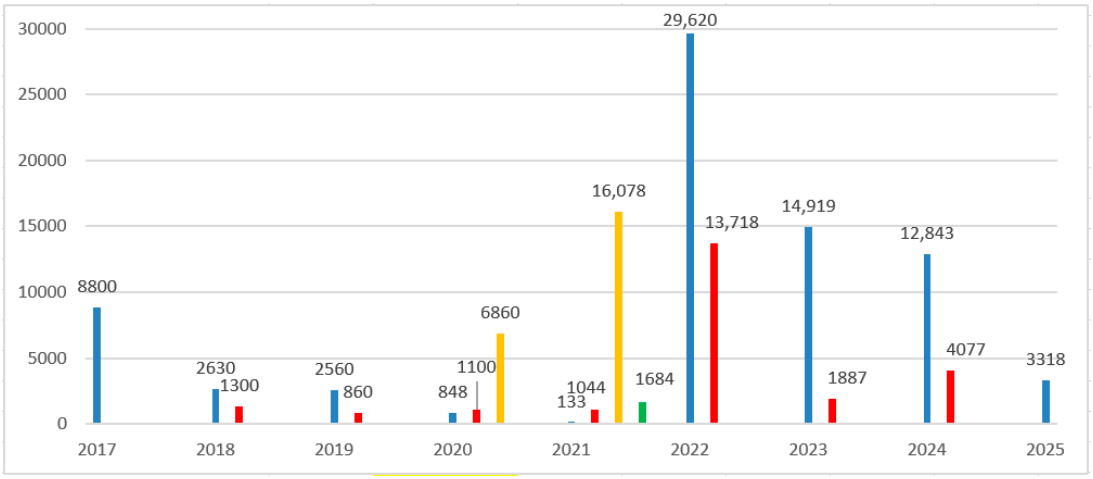

Figure 5. Year distribution of the datasets. For years with 2–3 data points, blue, red, yellow, and green mark the first, second, third, and forth entries, respectively. These colors serve only to distinguish data points and do not indicate any temporal sequence within the year.

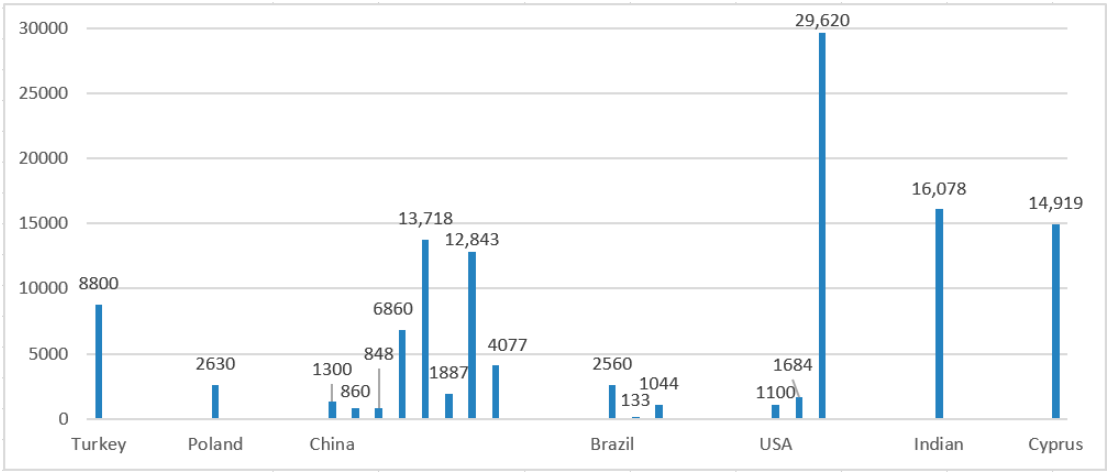

Figure 6. Location distribution of the datasets.

3.1.3. Image Resolution and Computational Trade-Offs

Image resolution dictates the granularity of spatial details, which is particularly critical for detecting miniature defects, such as missing pins or broken strands, against complex backgrounds. As shown in Figure 7, there is no standardized resolution across the domain. Dataset resolutions range from heavily down-sampled patches (e.g., 128 × 128 pixels in Yetgin's dataset) to ultra-high-definition multi-scale images (e.g., reaching 5472 × 3648 in STN PLAD or 4K in TTPLA). A critical challenge arises from multi-scale datasets where resolutions vary significantly even within the same repository, which is shown in Figure 8. While ultra-high-resolution images flawlessly preserve the morphological features of small power line components, they impose severe memory constraints and computational bottlenecks during both the training and inference phases. Consequently, researchers are often forced to resort to aggressive cropping or down-sampling, which inevitably risks information loss for small-scale targets. Balancing resolution fidelity with computational efficiency remains an open challenge in dataset utilization.

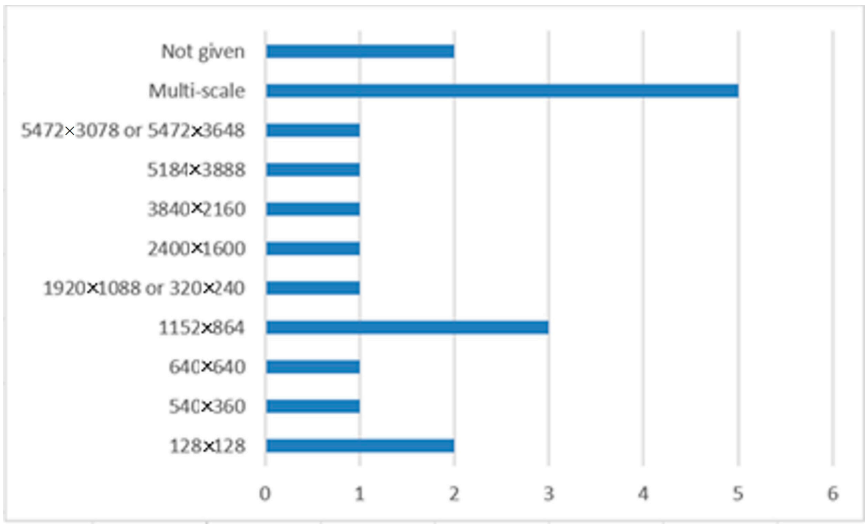

Figure 7. Resolution of the datasets.

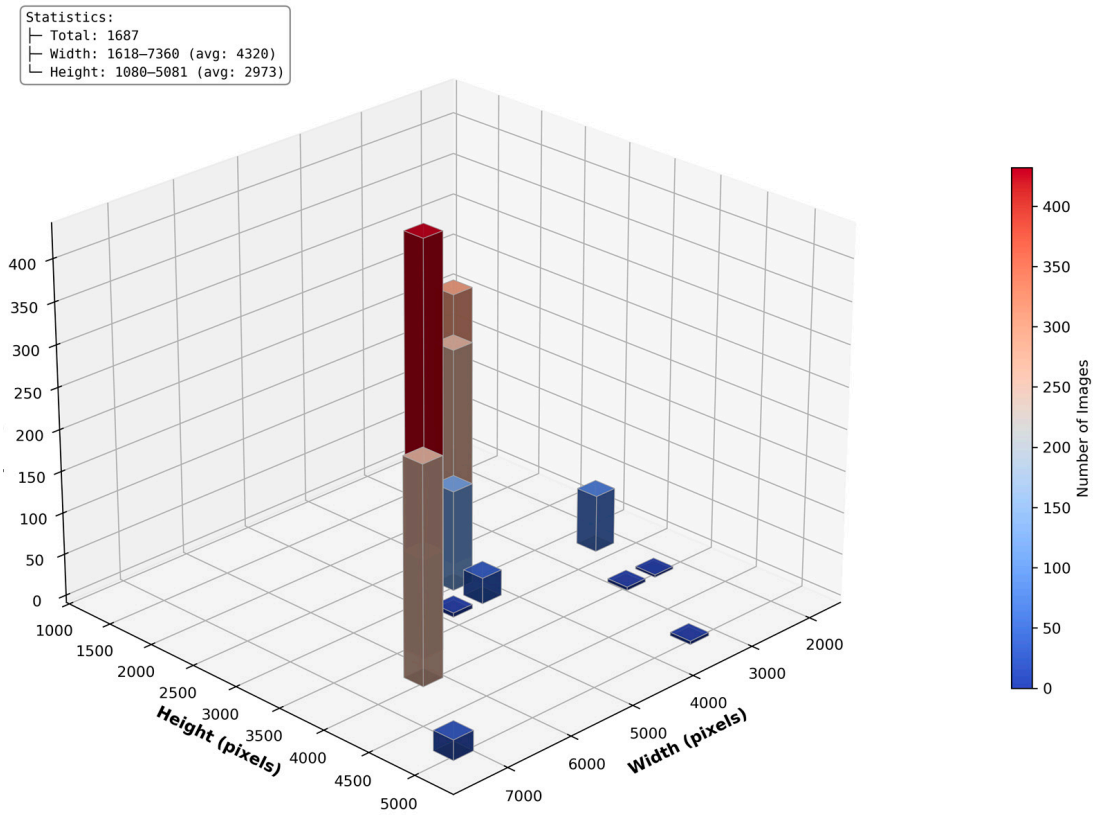

Figure 8. Resolution distributions of EPRI IDID.

3.2. Inspection Targets

These datasets are primarily captured around key power line components, including towers, conductors, insulators, spacers, dampers, plates, and transformers. To provide a systematic taxonomy of the inspection targets, the 19 reviewed datasets are categorized into four main groups: towers, conductors, insulators, and multiple targets/fittings, as summarized in Table 2. Dataset sizes vary considerably across these categories, ranging from roughly one hundred images to over ten thousand. Based on the statistical analysis shown in Figure 9, a critical observation emerges: there is a significant imbalance in data availability across different component types.

Table 2. Categorization of the reviewed datasets based on inspection targets.

Target	Count	Datasets	Key Characteristics
Tower	2	Bian's PTT, Savva's dataset	Large-scale grid structures. Challenges lie in identifying structural deformation or missing bolts.
Conductor	6	Yetgin's dataset, OPDL, PLD-UAV, Diniz's PTL, Pussente's PTL, Diwakar's dataset	Thin linear structures, highly susceptible to complex background interference (e.g., roads, branches).
Insulator	8	Tomaszewski'sdataset, CPLID, UPID, EPRI IDID, SFID, RSIn-dataset, DINS, ID-2024	Distinct periodic structure, easy to detect and annotate. Dominates the research field.
Multiple targets/fittings	3	TTPLA, STN PLAD, EPRI distribution inspection imagery	Extremely scarce. Includes small and diverse components (dampers, spacers, plates), demanding high-resolution data.

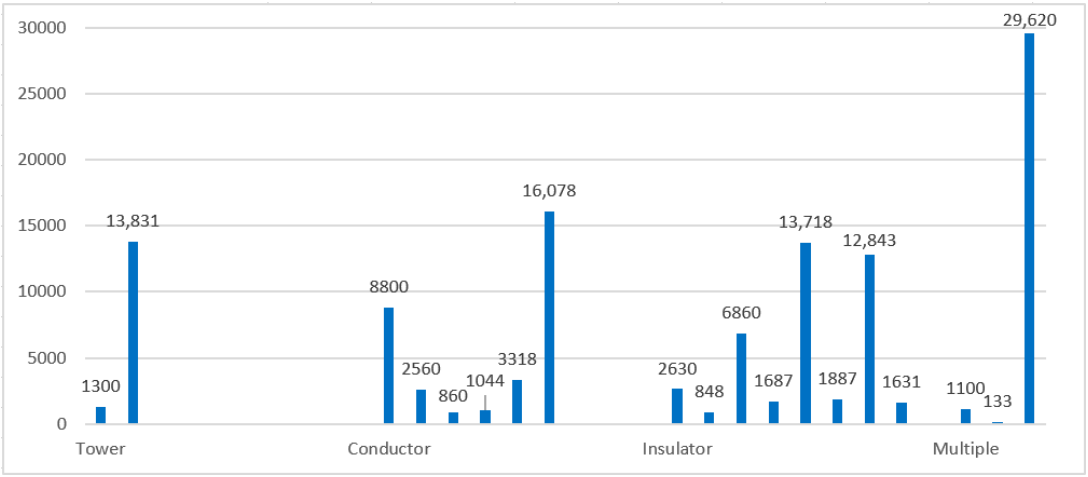

Figure 9. Target distribution of the datasets.

Insulator-focused datasets dominate the research field, accounting for nearly half of the available resources. This predominance is largely driven by two main factors. From a practical engineering perspective, insulators are highly vulnerable components whose failure can lead to severe consequences, such as flashovers and widespread power outages. Due to the need for frequent maintenance and replacement, they have traditionally been the primary focus during routine manual and drone-based inspections, resulting in an abundance of raw visual data. From a computer vision perspective, insulators possess highly distinctive and repetitive geometric shapes and textures. These physical characteristics make them relatively easier for both human annotators to label and detection algorithms to extract.

Conversely, datasets dedicated to conductors, towers, and especially small fittings (e.g., dampers, spacers, and pins) remain remarkably scarce. The lack of conductor datasets stems from their thin, linear structures, which easily blend into complex backgrounds like roads or vegetation, making accurate boundary annotation highly challenging. Furthermore, small hardware fittings suffer from extreme intra-class diversity and typically occupy only a minute fraction of pixels in aerial imagery. Consequently, collecting and labeling high-quality multi-target datasets, such as STN PLAD and EPRI distribution inspection imagery, demands significantly higher-resolution cameras and immense manual effort. This severe imbalance highlights an urgent need for the research community to shift its focus from the well-explored domain of insulator detection towards constructing comprehensive, high-quality datasets for conductors, towers, and diverse hardware fittings.

3.3. Data Acquisition Platforms and Paradigms

The methodology of image acquisition governs the viewpoint, coverage, and environmental diversity of power line inspection datasets. To provide a rigorous taxonomy, the reviewed datasets can be categorized based on their technical paradigms into three distinct physical platforms—dedicated systems, helicopters, and UAVs—supplemented by a digital simulation paradigm (Albumentations API). As illustrated in Figure 10, a clear chronological evolution exists from early infrastructure-dependent setups to highly autonomous, flexible mobile platforms.

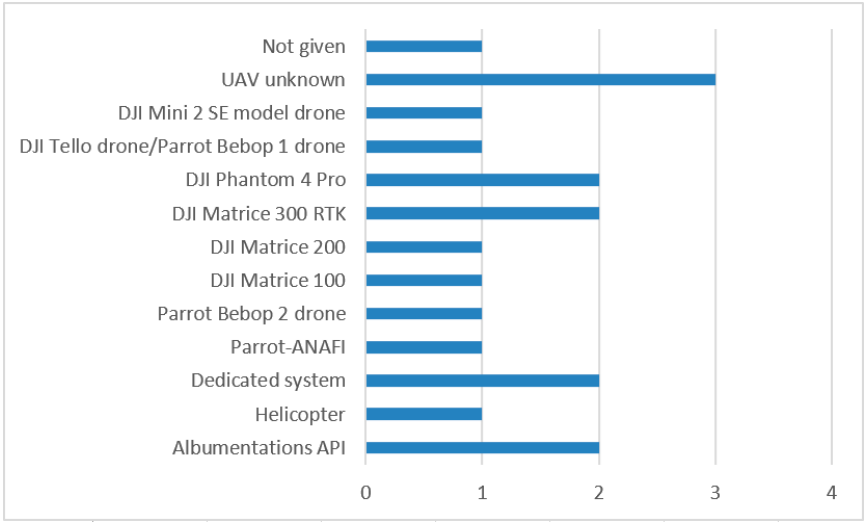

Figure 10. Platform distribution of the datasets.

It is clinically vital to clarify that while multi-modal imaging technologies such as infrared thermography, ultraviolet corona detection, and LiDAR point clouds are extensively deployed in routine real-world grid operations, their presence within open-access academic repositories remains severely limited. This critical deficit is strictly driven by stringent power grid security regulations and proprietary data privacy policies, meaning that although substantial multi-modal datasets exist internally within utility corporations, they are heavily restricted and remain entirely unreleased to the public research community.

3.3.1. Dedicated Systems

Early datatset collection primarily relied on dedicated experimental systems constructed in laboratory-controlled environments to mitigate the difficulties of real-grid sampling. For instance, Tomaszewski's insulator dataset utilized an aluminum frame outdoors under manually managed illumination angles, while Prates's OPDL dataset es-

tablished an image collection station (ICS) combined with a 30 m didactic overhead power line to systematically capture images. Although these systems offer unparalleled control over lighting and camera parameters, they inherently suffer from a "domain gap". The clean, repetitive backgrounds of laboratory setups fail to simulate the complex vegetation, varying terrains, and unpredictable clutter encountered in real-world grid operations, thereby limiting the robustness of models trained on them.

3.3.2. Helicopter-Based Airborne Systems

To capture real-world operational data across long-range transmission corridors, manned helicopters equipped with specialized airborne imaging systems have historically been deployed. A representative example is Yetgin's dataset, acquired in collaboration with the Turkish Electricity Transmission Company (TEIAS) using a helicopter-mounted multi-sensor pod containing both infrared (IR) and visible light (VL) cameras. Helicopter platforms excel in persistent, stable, and large-scale monitoring over hundreds of kilometers. However, their widespread academic and routine industrial adoption is strictly bottlenecked by exorbitant operational costs, high personnel safety risks, and the inability to perform ultra-close-range, multi-angle diagnostic hovering around single components.

3.3.3. UAVs

Over the past decade, commercially available multi-rotor UAVs have revolutionized power line inspection, becoming the mainstream platform for dataset construction. As summarized in Table 1 and Figure 10, off-the-shelf drones from DJI and Parrot dominate modern data acquisition. Drones successfully bridge the gap between macro-coverage and micro-details. For example, Bian's custom DJI Matrice 100 platform incorporates onboard computational nodes NVIDIA TX2/TK1 and intelligent pan-tilt cameras to dynamically track towers, as shown in Figure 11, while Abdelfatta's TTPLA dataset leverages 4K HDR lossless zoom capabilities from the Parrot ANAFI drone. UAVs provide cost-effective, multi-angle, and high-resolution imaging from close proximity. Nevertheless, they introduce unique data challenges, such as motion blur caused by aerodynamic vibrations and erratic viewpoint variations that complicate standardized bounding-box annotations.

3.3.4. Digital Data Augmentation Paradigm

Recognizing that physical platforms face severe regulatory and safety hurdles when capturing rare, critical fault images, recent paradigms have incorporated software-driven data generation to expand small-scale data footprints. The Albumentations API and custom synthetic networks represent the premier algorithmic tools used to artificially bolster dataset volume. Rather than merely providing descriptive accounts, a critical analysis of the literature reveals that these augmentation strategies yield substantial quantitative improvements in detection and classification performance.

For background fusion paradigms in CPLID, as shown in Figure 12, segmenting defective insulator patches and blending them onto diverse natural backgrounds provides critical semantic context for deep networks. Based on the experimental benchmarks in Ref. [45], when training a defect detector network on the fused augmented dataset, the precision surged from 62.58% to 94.19%. Weather-specific simulation offers unique algorithmic gains in hostile environments. In Zhang's SFID, generating synthetic fog under varying brightness levels (L: 0.1 to 0.9) and thicknesses (D: 0.01 to 0.09) via the Foggy Insulator Network (FINet) directly targets the domain degradation problem. Quantitative evaluation in Ref. [71] validates that models trained with a fog-containing dataset achieved 2.7% improvement in F1 score when tested on fog inspection scenes compared to models trained on a fog-free dataset. These quantitative insights conclusively prove that data

augmentation is not merely a descriptive scaling tool but a mathematical necessity for upgrading the boundary decision reliability of modern power line inspection models.



(**a**)

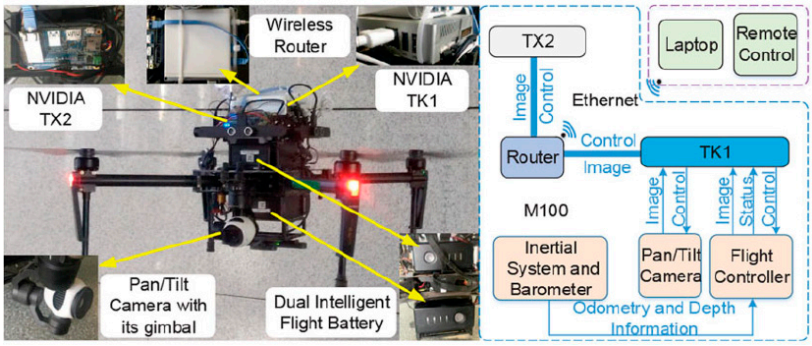

(**b**)

Figure 11. Evolution of platforms from dedicated system to commercial drones. (**a**) Research scenes of Tomaszewski's insulator dataset [30]. (**b**) Architecture of the inspection system of Bian's PTT dataset [35].

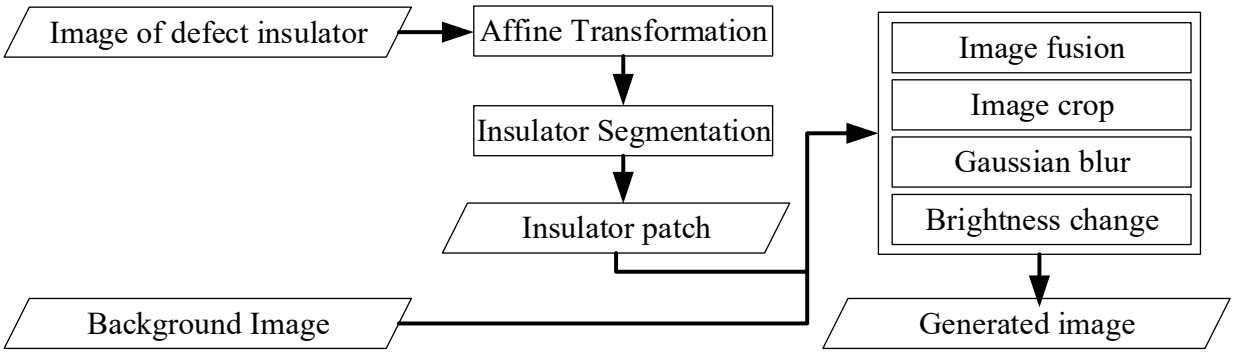

Figure 12. Data augmentation strategies.

Generally, the datasets were acquired in four kinds of platforms: Albumentations API, helicopters, dedicated systems, and UAVs. Specifically, Tomaszewski's insulator dataset and Prates's OPDL dataset were captured utilizing the dedicated systems in the laboratory-controlled environments. The remaining datasets were acquired with commercially available platforms. As shown in Figure 10, off-the-shelf UAVs are utilized for power line inspection, predominantly from DJI and Parrot.

3.4. Annotation Toolkit

The dataset labeling process represents a primary bottleneck in constructing supervised models for power line inspection, demanding extensive manual labor even with open-source annotation toolkits. Web-based or standalone platforms, such as LabelMe, LabelImg, computer vision annotation tool (CVAT), and Roboflow, are widely deployed in academic research. As illustrated in Figure 13, the annotation paradigms utilized in these

toolkits primarily bifurcate into coarse-grained bounding boxes and fine-grained polygon or pixel-wise masks, each presenting distinct computational and annotation trade-offs.

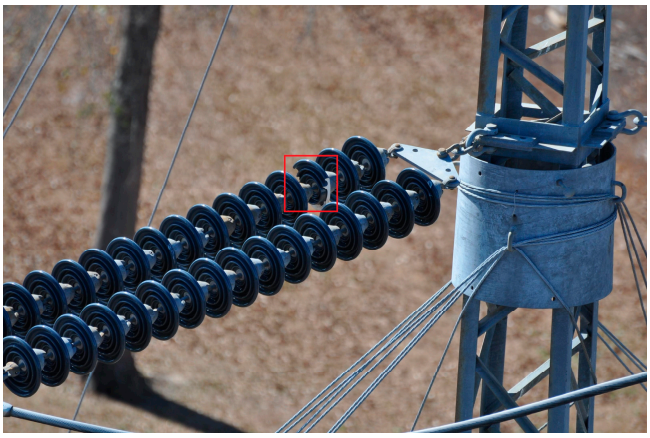

(**a**)

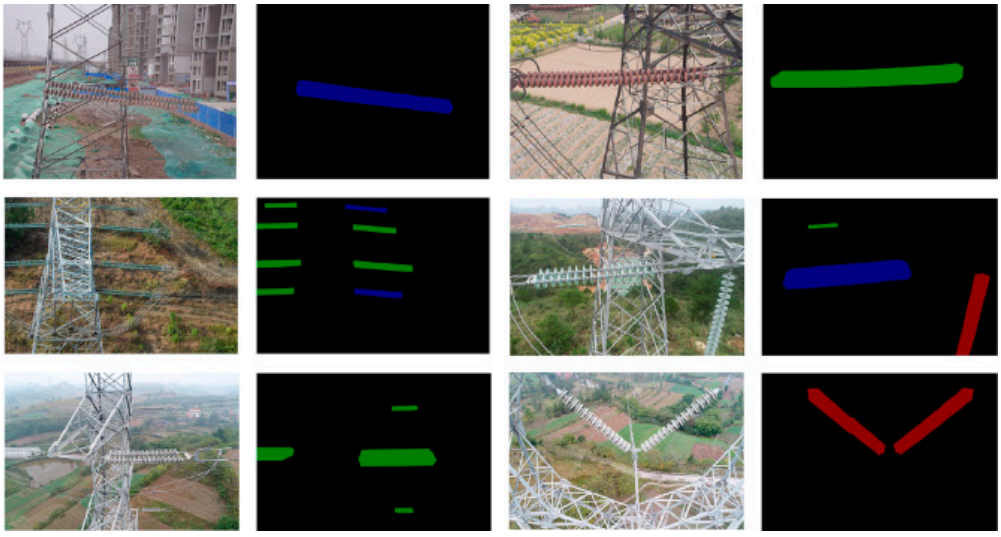

(**b**)

Figure 13. Polygon or pixel-wise masks. (**a**) Bounding box annotation. (**b**) Insulators and RGB-colored masks of DINS [80].

Bounding box annotations are typically formatted in Pascal VOC or YOLO schemes. They localize target components using rigid rectangular coordinates. This paradigm features low annotation complexity, making it highly suitable for rapidly expanding large-scale baseline repositories. However, bounding boxes inevitably incorporate significant background clutter inside the rectangle. For complex anomalies like missing insulator caps or minor rust spots, this background noise dilutes the texture features, introducing semantic ambiguity during deep neural network convergence.

Conversely, polygon or pixel-wise masks are typically formatted in MS COCO or semantic segmentation PNGs. They delineate the exact morphological boundaries of assets like conductors or multi-material insulators. The distinct advantage of this fine-grained paradigm is that it excludes background interference, allowing algorithms to perform pixel-level semantic extraction. Nevertheless, as validated by multi-task repositories, polygon labeling introduces an exponential increase in annotation time and strict human fatigue. For thin linear assets like conductors or microscopic details like component missing pins, accurate pixel placement demands ultra-high-resolution data inputs, directly

causing a critical engineering trade-off between semantic precision and the immense cost of manual annotation.

3.5. Dataset Labels

The diagnostic capability of a power line inspection model is strictly bounded by the granularity and semantic depth of its dataset labels. The labeling schemes of these datasets can be systematically classified into three escalating semantic levels: Component Level, Subcategory Level, and Fault-Diagnosis Level. This structured label taxonomy, along with explicit class examples from representative datasets, is detailed in Table 3.

Table 3. Granularity of labeling schemes in representative datasets.

Labeling Granularity	Target Class	Datasets	Explicit Label Examples
Component Level	Generic Infrastructure	STN PLAD	tower, insulator, spacer, damper, plate
		EPRI distribution inspection imagery	insulator, conductor, other_wire, pole, crossarm, guy_wires, transformers, background_structure, cutouts
Subcategory Level	Material and Spatial Configurations	TTPLA	cable, tower-lattice, tower-tucohy, tower-wooden
		DINS	glass_insulator, porcelain_insulator, single-string, double-string
Fault-Diagnosis Level	Anomaly and Defect States	CPLID	Insulator, defect
		UPID	normal insulator, defective insulators, insulators fault
		EPRI IDID	insulator string, flashover damage insulator shell, broken insulator shell, good insulator shell

The component-level label is the most fundamental paradigm. It utilizes generic asset names as semantic classes to support basic localization tasks, such as “insulator”, “tower”, “conductor”, and “fitting”. While highly standardized, these coarse labels fail to capture specialized technical variations. To resolve this, multi-component benchmarks like TTPLA upgrade this granularity by categorizing transmission lines as “cable” and classifying structural towers into distinct materials such as “tower-lattice”, “tower-tucohy”, and “tower-wooden”. The subcategory-level labels incorporate subcategory distinctions based on component materials or structural configurations to reduce intra-class variance during deep neural network convergence. A representative baseline is DINS, which applies unique RGB-colored segmentation masks to explicitly separate “glass insulator” and “porcelain insulator”, while differentiating “single-string” versus “double-string” spatial configurations. This fine-grained morphologic labeling is technically vital for preventing models from generating false positives under mixed industrial environments. The fault-diagnosis labels directly describe abnormal component health conditions rather than mere presence. As showcased by CPLID [45–47], UPID, and EPRI IDID, labels enrich bounding boxes with diagnostic classes such as “normal insulator”, “defective insulators”, and “insulators fault”.

In conclusion, while fine-grained and diagnostic labels are highly valuable for practical deployment, they remain remarkably scarce. Standardizing a community-consensus

naming convention and balancing diagnostic fault granularities remain the most pressing prerogatives for future dataset construction.

3.6. Recommended Applications

To provide a clear guideline for researchers, a comprehensive comparison of representative datasets is summarized in Table 4. While existing datasets have significantly advanced the field, their applicability is strictly governed by a trade-off between image quantity, spatial resolution, and computational burden. Early benchmark datasets like CPLID are excellent for basic insulator detection but suffer from limited image scale and background monotonicity. Conversely, massive datasets like the EPRI distribution inspection imagery offer unprecedented environmental diversity but impose heavy computational loads during the training and inference phases.

Table 4. Comparison of representative open-access datasets in power line inspection.

Dataset	Modality	Annotations	Characteristics	Recommended Applications
Yetgin's dataset	RGB, IR	Pixel-wise	Relatively early dataset of conductor.	Multi-modal image fusion; IR-based anomaly detection.
CPLID	RGB	Bounding box (VOC)	Widely recognized benchmark of insulator defect.	Insulator defect detection; few-shot learning.
TTPLA	RGB	Pixel-wise (COCO)	High resolution; covers towers and cables.	Instance/semantic segmentation of towers and conductors.
STN PLAD	RGB	Bounding box (COCO)	High resolution; small scale; covers diverse and rare small fittings.	Zero-shot or few-shot learning for small hardware/fittings.
EPRI distribution inspec-tion im-agery	RGB	Pixel-wise	High resolution; massive scale; rich diversity of distribution infrastructure.	Large-scale pre-training; semantic segmentation.
SFID	RGB	Bounding box (COCO)	Offers various synthetic fog thicknesses and brightness levels.	Dehazing algorithms; object detection under adverse weather.
DINS	RGB	Bounding box and pixel-wise	Large scale; focuses exclusively on insulators.	Joint detection and segmentation for insulators.

A critical nuance often overlooked is that dataset utility cannot be judged solely by the absolute image count. Several repositories appear small in terms of image volume but feature ultra-high resolutions and massive instance densities. For instance, datasets like STN PLAD contain only 133 images, yet their 5K high-fidelity resolution ensures that a single frame captures multiple fine-grained fittings with pixel-level precision. This high spatial fidelity makes them invaluable for few-shot learning research targeting rare small assets like dampers and spacers. Similarly, TTPLA leverages 4K resolution to pack thousands of localized asset instances into just over one thousand frames, supporting high-density instance segmentation. For data-hungry state-of-the-art networks, these

high-resolution repositories are not only for from-scratch optimization but also serve as high-quality benchmarks for transfer learning, micro-defect fine-tuning, and cross-domain validation.

Furthermore, specialized datasets cater to specific niche challenges in the power domain. SFID is highly effective for evaluating algorithm robustness under adverse weather conditions, provided that researchers remain cautious of the domain gap between synthetically generated fog and real operational environments. Ultimately, the choice of dataset must strictly align with the specific downstream engineering task, whether it requires multi-modal image fusion using Yetgin's IR and VL, high-density instance segmentation using TTPLA and DINS, or fine-grained anomaly detection using specialized small-scale benchmarks.

4. Conclusions

The continuous evolution of open-access repositories has significantly catalyzed algorithmic innovation in automated power line inspection. Although recent benchmarks demonstrate a trajectory toward larger volumes, a substantial portion of existing datasets remains restricted in scale, frequently suffering from constrained environmental diversity and severe class imbalances. Geographically, data collection exhibits a heavy concentration within China, followed by emerging contributions from Brazil and the United States. While this multi-national engagement underscores the global urgency of deploying intelligent grid maintenance, it inherently introduces geospatial and background biases. Furthermore, structural target imbalances persist across the literature, where the over-recycled focus on insulator diagnostics leaves critical infrastructures like transmission towers, conductors, and hardware fittings heavily under-represented, thereby demanding broad-scale dataset diversification. Concurrently, standardizing metadata annotations remains a critical bottleneck. The vast majority of open-access data is restricted to coarse-grained bounding boxes for object detection, whereas high-fidelity repositories supporting instance segmentation or fine-grained fault classification are remarkably scarce. This architectural deficit is further compounded by severe variances in annotation quality and a complete lack of a universally adopted consensus for naming component subcategories or diagnostic fault types. Moving forward, the curation of high-quality, standardized benchmarks will dictate the ultimate operational reliability of autonomous deep learning deployment across real-world transmission networks.

To fully unlock the potential of autonomous aerial grid diagnostic frameworks, future research must systematically overcome these data-centric bottlenecks. Enhancing model generalization requires a concerted expansion of datasets to encompass extreme meteorological conditions [86], highly complex terrains, and the full morphological spectrum of grid hardware [87]. Concurrently, the operational energy constraints and power management architectures of deploying UAVs [88,89] must be integrated into algorithmic design to balance onboard computational efficiency with data capture rates. Transitioning from rudimentary target localization to industrial-grade fault diagnosis [90] through advanced digital twins for power asset management [91] inherently hinges on enriching these repositories with fine-grained, pixel-level semantic masks to facilitate precision cyber–physical alignment. To resolve the persistent bottleneck of long-tail fault distributions where authentic failure data is natively scarce, the generative synthesis of high-fidelity artificial images represents a pivotal frontier. Ultimately, forging a community-consensus annotation standard is the most pressing prerequisite to enable cross-dataset transfer learning and fair algorithmic benchmarking. In summary, while public data has successfully propelled the initial wave of vision-based inspections, realizing fully autonomous, field-ready grid surveillance re-

quires a coordinated paradigm shift toward high-quality, standardized, and diversity-rich data engineering.

Author Contributions: Conceptualization, X.-H.W. and Y.-Q.B.; methodology, X.-H.W.; investigation, E.Z. and K.Y.; writing—original draft preparation, X.-H.W.; writing—review and editing, Y.-Q.B. All authors have read and agreed to the published version of the manuscript.

Funding: This work was supported by the Start-up Fund for New Talented Researchers of Nanjing University of Industry Technology (Grant No. YK22-02-05).

Data Availability Statement: No new data was created or analyzed in this study.

Acknowledgments: The authors thank the contributors and maintainers of the public datasets used in this study for making their valuable resources openly available to the research community.

Conflicts of Interest: The authors declare no conflicts of interest. The funders had no role in the design of the study; in the collection, analyses, or interpretation of data; in the writing of the manuscript; or in the decision to publish the results.

Nomenclature

CNN	Convolutional neural networks
CPLID	Chinese power line insulator dataset
CSV	Comma-Separated Values
CVAT	Computer Vision Annotation Tool
DNN	Deep neural networks
GPS	Global positioning system
GTD	Ground-truth data
IDID	Insulator defect image dataset
IMU	Inertial measurement unit
IR	Infrared
JSON	Java Script Object Notation
LiDAR	Light Detection and Ranging
MS	COCO Microsoft Common Objects in Context
OPDL	Overhead power distribution lines.
PASCALVOC	Pattern analysis, statical modeling, and computational learning visual object classes
PLD-UAV	Power line detection in unmanned aerial vehicles
PTL	Power transmission line
PTT	Power transmission tower
PTC	Pan/Tilt camera
SSD	Single shot multibox detector
SVM	Support vector machine
TEIAS	Turkish electricity transmission corporation
TR	Track-mounted robots
TTPLA	Transmission towers and power lines
UAV	Unmanned aerial vehicles
UPID	Unifying public datasets for insulator
VL	Visible light
YOLO	You only look once

References

1. Everingham, M.; Van Gool, L.; Williams, C.K.I.; Winn, J.; Zisserman, A. The Pascal Visual Object Classes (VOC) Challenge. *Int. J. Comput. Vis.* **2010**, *88*, 303–338. [CrossRef]
2. Deng, J.; Dong, W.; Socher, R.; Li, L.-J.; Li, K.; Li, F.-F. ImageNet: A large-scale hierarchical image database. In Proceedings of the 2009 IEEE Conference on Computer Vision and Pattern Recognition, Miami, FL, USA, 20–25 June 2009; pp. 248–255. [CrossRef]

3. Lin, T.Y.; Maire, M.; Belongie, S.; Hays, J.; Perona, P.; Ramanan, D.; Dollár, P.; Zitnick, C.L. Microsoft COCO: Common Objects in Context. In *Computer Vision—ECCV 2014*; Fleet, D., Pajdla, T., Schiele, B., Tuytelaars, T., Eds.; Springer: Cham, Switzerland, 2014; Volume 8693. [CrossRef]
4. Kuznetsova, A.; Rom, H.; Alldrin, N.; Uijlings, J.; Krasin, I.; Pont-Tuset, J.; Kamali, S.; Popov, S.; Malloci, M.; Kolesnikov, A.; et al. The Open Images Dataset V4. *Int. J. Comput. Vis.* **2020**, *128*, 1956–1981. [CrossRef]
5. Voigt, P.; Von dem Bussche, A. The EU general data protection regulation (GDPR). In *A Practical Guide*, 1st ed.; Springer International Publishing: Cham, Switzerland, 2017; Volume 10, pp. 9–36.
6. Hao, Y.; Liang, W.; Pan, R.; Luo, B.; Li, L.; Zhang, F.; Wang, T. Review on intelligent live-line maintenance technology applied on power transmission lines. *Electr. Power Autom. Equip.* **2022**, *42*, 163–175.
7. Yang, L.; Fan, J.; Liu, Y.; Li, E.; Peng, J.; Liang, Z. A Review on State-of-the-Art Power Line Inspection Techniques. *IEEE Trans. Instrum. Meas.* **2020**, *69*, 9350–9365. [CrossRef]
8. Liu, X.; Miao, X.; Jiang, H.; Chen, J. Data analysis in visual power line inspection: An in-depth review of deep learning for component detection and fault diagnosis. *Annu. Rev. Control* **2020**, *50*, 253–277. [CrossRef]
9. Zhou, F.; Jin, W.; Zheng, Z.; Mou, F.; Li, Z.; Ma, Y.; Wei, B.; Huang, S.; Wang, Q. Insulator detection for high-resolution satellite images based on deep learning. *IEEE Geosci. Remote Sens. Lett.* **2023**, *20*, 5001105. [CrossRef]
10. Jaffery, Z.A.; Dubey, A.K. Design of early fault detection technique for electrical assets using infrared thermograms. *Int. J. Electr. Power Energy Syst.* **2014**, *63*, 753–759. [CrossRef]
11. Singh, L.; Alam, A.; Kumar, K.V.; Kumar, D.; Kumar, P.; Jaffery, Z.A. Design of thermal imaging-based health condition monitoring and early fault detection technique for porcelain insulators using machine learning. *Environ. Technol. Innov.* **2021**, *24*, 102000. [CrossRef]
12. Hu, B.; Ma, L.-X.; Yuan, S.-J.; Yang, B. New corona ultraviolet detection system and fault location method. In Proceedings of the 2012 China International Conference on Electricity Distribution, Xiamen, China, 10–14 September 2012; pp. 1–4. [CrossRef]
13. Li, Y.; Yu, F.; Cai, Q.; Yuan, K.; Wan, R.; Li, X.; Qian, M.; Liu, P.; Guo, J.; Yu, J.; et al. Image fusion of fault detection in power system based on deep learning. *Clust. Comput.* **2019**, *22*, 9435–9443. [CrossRef]
14. Zang, C.; He, J.; Yin, X.; Chen, B.; Lei, H.; Jiang, Z.; Zhao, X. Status and application foreground of ultraviolet technology on fault detection of power devices. In Proceedings of the 2008 International Conference on Condition Monitoring and Diagnosis, Beijing, China, 21–24 April 2008; pp. 122–125. [CrossRef]
15. Guan, H.; Sun, X.; Su, Y.; Hu, T.; Wang, H.; Wang, H.; Peng, C.; Guo, Q. UAV-lidar aids automatic intelligent powerline inspection. *Int. J. Electr. Power Energy Syst.* **2021**, *130*, 106987. [CrossRef]
16. Bergmann, M.A.; Moreira, L.F.R.; Krohling, B.; Silveira, T.L.; Jung, C.R.; Tang, J.; Feitosa, M.V.; Gomes, R.L.B.; Soares, B.N. An approach based on LiDAR and spherical images for automated vegetation inspection in urban power distribution lines. *IEEE Access* **2024**, *12*, 105119–105130. [CrossRef]
17. Wang, F.; Song, G.; Mao, J.; Li, Y.; Ji, Z.; Chen, D.; Song, A. Internal defect detection of overhead aluminum conductor composite core transmission lines with an inspection robot and computer vision. *IEEE Trans. Instrum. Meas.* **2023**, *72*, 3512516. [CrossRef]
18. Faisal, M.A.A.; Mecheter, I.; Qiblawey, Y.; Fernandez, J.H.; Chowdhury, M.E.H.; Kiranyaz, S. Deep learning in automated power line inspection: A review. *Appl. Energy* **2025**, *385*, 125507. [CrossRef]
19. Jocher, G.; Chaurasia, A.; Qiu, J. Ultralytics YOLO. 2023. Available online: https://github.com/ultralytics/ultralytics (accessed on 19 April 2026).
20. Liu, Y.; Liu, D.; Huang, X.; Li, C. Insulator defect detection with deep learning: A survey. *IET Gener. Transm. Distrib.* **2023**, *17*, 3541–3558. [CrossRef]
21. Lee, S.J.; Yun, J.P.; Choi, H.; Kwon, W.; Koo, G.; Kim, S.W. Weakly supervised learning with convolutional neural networks for power line localization. In Proceedings of the 2017 IEEE Symposium Series on Computational Intelligence (SSCI), Honolulu, HI, USA, 27 November–1 December 2017; pp. 1–8.
22. Yetgin, Ö.E.; Gerek, Ö.N. Powerline Image Dataset (Infrared-IR and Visible Light-VL). *Mendeley Data* **2017**, *v3*. Available online: https://data.mendeley.com/datasets/n6wrv4ry6v/3.
23. Yetgin, Ö.E.; Gerek, Ö.N. Ground Truth of Power Line Dataset (Infrared-IR and Visible Light-VL). *Mendeley Data* **2017**, *v6*. Available online: https://data.mendeley.com/datasets/twxp8xccsw/6.
24. Yetgin, Ö.E.; Gerek, Ö.N. Powerline Image Dataset Extra (Infrared-IR and Visible Light-VL)-Classified (Easy and Hard). Mendeley Data, v7. 2017. Available online: https://data.mendeley.com/datasets/n6wrv4ry6v/7 (accessed on 19 April 2026).
25. Yetgin, Ö.E. Powerline Image Dataset (Infrared-IR and Visible Light-VL). 2017. Available online: https://data.mendeley.com/datasets/n6wrv4ry6v/8 (accessed on 19 April 2026).
26. Yetgin, Ö.E.; Gerek, Ö.N. Ground Truth of Powerline Dataset (Infrared-IR and Visible Light-VL). *Mendeley Data* **2019**, *v9*. Available online: https://data.mendeley.com/datasets/twxp8xccsw/9.

27. Yetgin, Ö.E.; Gerek, Ö.N. A comparison of corner and saliency detection methods for power line detection. In Proceedings of the 2017 International Artificial Intelligence and Data Processing Symposium (IDAP), Malatya, Turkey, 16–17 September 2017; pp. 1–5. [CrossRef]
28. Yetgin, Ö.E.; Gerek, Ö.N. Automatic recognition of scenes with power line wires in real life aerial images using DCT-based features. *Digit. Signal Process.* **2017**, *77*, 102–119. [CrossRef]
29. Yetgin, Ö.E.; Benligiray, B.; Gerek, Ö.N. Power line recognition from aerial images with deep learning. *IEEE Trans. Aerosp. Electron. Syst.* **2019**, *55*, 2241–2252. [CrossRef]
30. Tomaszewski, M.; Ruszczak, B.; Michalski, P. The collection of images of an insulator taken outdoors in varying lighting conditions with additional laser spots. *Data Brief.* **2018**, *18*, 765–768. [CrossRef] [PubMed]
31. Tomaszewski, M.; Michalski, P.; Ruszczak, B.; Zator, S. Detection of power line insulators on digital images with the use of laser spots. *IET Image Process.* **2019**, *13*, 2358–2366. [CrossRef]
32. Ruszczak, B.; Michalski, P.; Tomaszewski, M. Overview of Image Datasets for Deep Learning Applications in Diagnostics of Power Infrastructure. *Sensors* **2023**, *23*, 7171. [CrossRef] [PubMed]
33. Dataset Repository. Available online: https://cv.po.opole.pl/dataset1 (accessed on 19 April 2026).
34. Bian, J.; Hui, X.; Zhao, X.; Tan, M. A Novel Monocular-Based Navigation Approach for UAV Autonomous Transmission-Line Inspection. In Proceedings of the 2018 IEEE/RSJ International Conference on Intelligent Robots and Systems (IROS), Madrid, Spain, 1–5 October 2018; pp. 1–7. [CrossRef]
35. Bian, J.; Hui, X.; Zhao, X.; Tan, M. A monocular vision–based perception approach for unmanned aerial vehicle close proximity transmission tower inspection. *Int. J. Adv. Robot. Syst.* **2019**, *16*, 1729881418820227. [CrossRef]
36. Hui, X.; Bian, J.; Zhao, X.; Tan, M. A monocular-based navigation approach for unmanned aerial vehicle safe and autonomous transmission-line inspection. *Int. J. Adv. Robot. Syst.* **2019**, 1–16. [CrossRef]
37. Google Drive Dataset. Available online: https://drive.google.com/drive/folders/1UyP0fBNUqFeoW5nmPVGzyFG5IQZcqlc5 (accessed on 19 April 2026).
38. Prates, R.M.; Cruz, R.; Marotta, A.P.; Ramos, R.P.; Filho, E.F.S.; Cardoso, J.S. Insulator visual non-conformity detection in overhead power distribution lines using deep learning. *Comput. Electr. Eng.* **2019**, *78*, 343–355. [CrossRef]
39. Freedman, D.; Zhang, T. Interactive graph cut based segmentation with shape priors. In Proceedings of the 2005 IEEE Computer Society Conference on Computer Vision and Pattern Recognition (CVPR'05), San Diego, CA, USA, 20–26 June 2005; pp. 755–762.
40. OPDL Dataset. Available online: http://www.dee.eng.ufba.br/dslab/index.php/opdl_dataset (accessed on 19 April 2026).
41. Zhang, H.; Yang, W.; Yu, H.; Zhang, H.; Xia, G.-S. Detecting Power Lines in UAV Images with Convolutional Features and Structured Constraints. *Remote Sens.* **2019**, *11*, 1342. [CrossRef]
42. Qin, X.; He, S.; Zhang, Z.; Dehghan, M. ByLabel: A Boundary Based Semi-Automatic Image Annotation Tool. In Proceedings of the IEEE Winter Conference on Applications of Computer Vision (WACV), Lake Tahoe, NV, USA, 12–15 March 2018; pp. 1804–1813.
43. Akinlar, C.; Topal, C. EDLines: A real-time line segment detector with a false detection control. *Pattern Recognit. Lett.* **2011**, *32*, 1633–1642. [CrossRef]
44. PLD-UAV GitHub Repository. Available online: https://github.com/SnorkerHeng/PLD-UAV (accessed on 19 April 2026).
45. Tao, X.; Zhang, D.; Wang, Z.; Liu, X.; Zhang, H.; Xu, D. Detection of power line insulator defects using aerial images analyzed with convolutional neural networks. *IEEE Trans. Syst. Man Cybern. Syst.* **2018**, *50*, 1486–1498. [CrossRef]
46. Unger, M.; Pock, T.; Trobin, W.; Cremers, D.; Bischof, H. TVSeg—Interactive Total Variation Based Image Segmentation. 2008. Available online: https://www.bmva-archive.org.uk/bmvc/2008/papers/208.html (accessed on 19 April 2026).
47. Ronneberger, O.; Fischer, P.; Brox, T. U-Net: Convolutional Networks for Biomedical Image Segmentation. In *Medical Image Computing and Computer-Assisted Intervention—MICCAI 2015*; Navab, N., Hornegger, J., Wells, W., Frangi, A., Eds.; Springer: Cham, Switzerland, 2015; p. 9351. [CrossRef]
48. InsulatorData GitHub Repository. Available online: https://github.com/InsulatorData (accessed on 19 April 2026).
49. Insulator Data Set (Chinese Power Line Insulator Dataset). Available online: https://ieee-dataport.org/open-access/insulator-data-set-chinese-power-line-insulator-dataset-cplid (accessed on 19 April 2026).
50. Abdelfattah, R.; Wang, X.; Wang, S. TTPLA: An Aerial-Image Dataset for Detection and Segmentation of Transmission Towers and Power Lines. In *Computer Vision—ACCV 2020*; Ishikawa, H., Liu, C.L., Pajdla, T., Shi, J., Eds.; Springer: Cham, Switzerland, 2021; Volume 12627. [CrossRef]
51. TTPLA Dataset GitHub Repository. Available online: https://github.com/R3ab/ttpla_dataset (accessed on 19 April 2026).
52. Google Drive Dataset Download. Available online: https://drive.google.com/uc?export=download&confirm=no_antivirus&id=1Yz59yXCiPKS0_X4K3x9mW22NLnxjvrr0 (accessed on 19 April 2026).
53. Vieira-e-Silva, A.L.; Chaves, T.; Felix, H.; Macêdo, D.; Simões, F.; Gama-Neto, M.; Teichrieb, V.; Zanchettin, C. Unifying Public Datasets for Insulator Detection and Fault Classification in Electrical Power Lines. GitHub 2020. Available online: https://github.com/heitorcfelix/public-insulator-datasets (accessed on 19 April 2026).

54. Buslaev, A.; Iglovikov, V.I.; Khvedchenya, E.; Parinov, A.; Druzhinin, M.; Kalinin, A.A. Albumentations: Fast and flexible image augmentations. *Information* **2020**, *11*, 125. [CrossRef]
55. Vieira-e-Silva, A.L.B.; de Castro Felix, H.; de Menezes Chaves, T.; Simoes, F.P.M.; Teichrieb, V.; dos Santos, M.M.; da Cunha Santiago, H.; Sgotti, V.A.C.; Neto, H.B.D.T.L. STN PLAD: A dataset for multi-size power line assets detection in high-resolution UAV images. In Proceedings of the 2021 34th SIBGRAPI Conference on Graphics, Patterns and Images, Gramado, Brazil, 25–29 October 2021; pp. 215–222. [CrossRef]
56. PLAD GitHub Repository. Available online: https://github.com/andreluizbvs/PLAD (accessed on 19 April 2026).
57. PLAD Dataset Download. Available online: https://github.com/andreluizbvs/PLAD/releases/download/1.0/plad.zip (accessed on 19 April 2026).
58. Google Drive Data Share. Available online: https://drive.google.com/file/d/1KsNziErZ5ZRuWBpwUS5nlTnb8CcB2uQp/view?usp=sharing (accessed on 19 April 2026).
59. PLAD Labels Download. Available online: https://github.com/andreluizbvs/PLAD/files/8952243/labels.zip (accessed on 19 April 2026).
60. Diniz, L.; Santa Maria, T.; Pussente, G.A. Power transmission line dataset. *IEEE Dataport* **2021**. [CrossRef]
61. Pussente, G.A.N.; Santa Maria, T.H.; Marcato, A.L.M.; de Aguiar, E.P. Trajectory Detection Method for Transmission Line Path Following Control. In Proceedings of the 2021 Latin American Robotics Symposium (LARS), 2021 Brazilian Symposium on Robotics (SBR), and 2021 Workshop on Robotics in Education (WRE), Natal, Brazil, 23–27 November 2021; pp. 42–47. [CrossRef]
62. Roboflow. Roboflow Open-Source Repositories. GitHub. 2026. Available online: https://github.com/roboflow (accessed on 19 April 2026).
63. Pussente, G.A.N.; Biundini, I.Z.; Marcato, A.L.M.; de Aguiar, E.P. Advanced drone-based powerline inspection using image segmentation and adaptive visual control. *J. Braz. Soc. Mech. Sci. Eng.* **2025**, *47*, 112. [CrossRef]
64. PL Inspection GitHub Repository. Available online: https://github.com/guiaugustoga987/pl_inspection (accessed on 19 April 2026).
65. Powerlines Dataset GitHub Repository. Available online: https://github.com/guiaugustoga987/powerlines_dataset (accessed on 19 April 2026).
66. Diwakar, T. (Recognizance—2) Power Lines Detection. Kaggle 2021. Available online: https://kaggle.com/competitions/recognizance-2 (accessed on 19 April 2026).
67. Lewis, D.; Kulkarni, P. Insulator Defect Detection. IEEE Dataport. 2021. Available online: https://ieee-dataport.org/competitions/insulator-defect-detection (accessed on 19 April 2026).
68. Lewis, D.; Kulkarni, P. EPRI Distribution Inspection Imagery. IEEE Dataport. 2021. Available online: https://ieee-dataport.org/open-access/epri-distribution-inspection-imagery (accessed on 19 April 2026).
69. Kickstarter Notebook Kaggle. Available online: https://www.kaggle.com/code/pratikkulkarniepri/kickstarter/notebook (accessed on 19 April 2026).
70. EPRI Distribution Inspection Imagery Kaggle. Available online: https://www.kaggle.com/datasets/dexterlewis/epri-distribution-inspection-imagery (accessed on 19 April 2026).
71. Zhang, Z.-D.; Zhang, B.; Lan, Z.-C.; Liu, H.-C.; Li, D.-Y.; Pei, L.; Yu, W.-X. FINet: An insulator dataset and detection benchmark based on synthetic fog and improved YOLOv5. *IEEE Trans. Instrum. Meas.* **2022**, *71*, 1–8. [CrossRef]
72. FINet GitHub Repository. Available online: https://github.com/zhangzhengde0225/FINet (accessed on 19 April 2026).
73. Savva, A.; Zacharia, A.; Makrigiorgis, R.; Anastasiou, A.; Kyrkou, C.; Kolios, P.; Panayiotou, C.; Theocharides, T. ICARUS: Automatic Autonomous Power Infrastructure Inspection with UAVs. In Proceedings of the 2021 International Conference on Unmanned Aircraft Systems (ICUAS), Athens, Greece, 15–18 June 2021; pp. 918–926. [CrossRef]
74. Savva, A.; Makrigiorgis, R.; Kolios, P.; Kyrkou, C. Aerial Power Infrastructure Detection Dataset. 2023. Available online: https://zenodo.org/records/7781388 (accessed on 19 April 2026).
75. Liu, X.; Li, Y.; Shuang, F.; Gao, F.; Zhou, X.; Chen, X. ISSD: Improved SSD for Insulator and Spacer Online Detection Based on UAV System. *Sensors* **2020**, *20*, 6961. [CrossRef]
76. Shuang, F.; Han, S.; Li, Y.; Lu, T. RSIn-dataset: An UAV-based insulator detection aerial images dataset and benchmark. *Drones* **2023**, *7*, 125. [CrossRef]
77. Li, Y.; Hu, B.; Zhu, W.; Feng, X.; Ye, T. Insulator and Spacer Dataset and Benchmark for Power Inspection. In Proceedings of the 2023 6th International Conference on Intelligent Autonomous Systems (ICoIAS), Qinhuangdao, China, 22–24 September 2023; pp. 41–46. [CrossRef]
78. RSIn-Dataset GitHub Repository. Available online: https://github.com/caigouyihao/Rsin-dataset (accessed on 19 April 2026).
79. Cui, B.; Han, C.; Yang, M.; Ding, L.; Shuang, F. DINS: A Diverse Insulator Dataset for Object Detection and Instance Segmentation. *IEEE Trans. Ind. Inform.* **2024**, *20*, 12252–12261. [CrossRef]
80. DINs GitHub Repository. Available online: https://github.com/beyondliberty/DINs (accessed on 19 April 2026).
81. Google Drive Data Share. Available online: https://drive.google.com/file/d/1NPAYjM99kRGda5aiBZBCK0rGdLewVYyE/view?usp=drive_link (accessed on 19 April 2026).

82. Lu, Y.; Li, D.; Li, D.; Li, X.; Gao, Q.; Yu, X. A Lightweight Insulator Defect Detection Model Based on Drone Images. *Drones* **2024**, *8*, 431. [CrossRef]
83. McCartney, E.J. Optics of the atmosphere: Scattering by molecules and particles. *Phys. Bull.* **1976**, *28*, 521. [CrossRef]
84. Narasimhan, S.G.; Nayar, S.K. Vision and the atmosphere. *Int. J. Comput. Vis.* **2002**, *48*, 233–254. [CrossRef]
85. Insulator-Defect-Detection-YOLO GitHub Repository. Available online: https://github.com/LuYang-2023/Insulator-Defect-Detection-YOLO?tab=readme-ov-file (accessed on 19 April 2026).
86. Kyem, B.A.; Asamoah, J.K.; Huang, Y.; Aboah, A. Weather-Adaptive Synthetic Data Generation for Enhanced Power Line Inspection Using StarGAN. *IEEE Access* **2024**, *12*, 193882–193901. [CrossRef]
87. Xu, C.; Li, Q.; Jiang, X.; Yu, D.; Zhou, Y. Dual-Space Graph-Based Interaction Network for RGB-Thermal Semantic Segmentation in Electric Power Scene. *IEEE Trans. Circuits Syst. Video Technol.* **2023**, *33*, 1577–1592. [CrossRef]
88. Citroni, R.; Leggieri, A.; Passi, D.; Di Paolo, F.; Di Carlo, A. Nano Energy Harvesting with Plasmonic Nano-Antennas: A review of MID-IR Rectenna and Application. *Adv. Electromagn.* **2017**, *6*, 1–13. [CrossRef]
89. Citroni, R.; Di Paolo, F.; Livreri, P. A Novel Energy Harvester for Powering Small UAVs: Performance Analysis, Model Validation and Flight Results. *Sensors* **2019**, *19*, 1771. [CrossRef]
90. Odo, A.; McKenna, S.; Flynn, D.; Vorstius, J.B. Aerial Image Analysis Using Deep Learning for Electrical Overhead Line Network Asset Management. *IEEE Access* **2021**, *9*, 146281–146295. [CrossRef]
91. Abongo, A.D.; Jaafar, W.; Langar, R. Generative AI-Assisted Digital Twin for Power Asset Management. *IEEE Commun. Mag.* **2025**, *63*, 46–52. [CrossRef]

Disclaimer/Publisher's Note: The statements, opinions and data contained in all publications are solely those of the individual author(s) and contributor(s) and not of MDPI and/or the editor(s). MDPI and/or the editor(s) disclaim responsibility for any injury to people or property resulting from any ideas, methods, instructions or products referred to in the content.